Matter-Wave–Optical-Wave Mixing-Induced Transparency and a Nonhyperbolic Matter-Wave Quasisoliton in Quantum Gases

Yan Li,[1] Chengjie Zhu,[2,*] W. R. Garrett,[3] E. W. Hagley,[4] and L. Deng[4,†]

[1]*Department of Physics, East China Normal University, Shanghai 200241, China*
[2]*MOE Key Laboratory of Advanced Micro-Structured Materials, School of Physics Science and Engineering,
Tongji University, Shanghai 200092, China*
[3]*Department of Physics, University of Tennessee, Knoxville, Tennessee 37996, USA*
[4]*National Institute of Standards and Technology, Gaithersburg, Maryland 20899, USA*

The realization of atomic quantum gases has brought out surprising effects that have no correspondence in nonlinear optics with thermal gases, presenting intriguing and exciting challenges to the research discipline of nonlinear optics which has matured since the invention of the laser. Here, we show an unexpected optical wave-mixing gain cancellation effect in a quantum gas that restricts an, otherwise, strongly enhanced backward-propagating light-matter wave-mixing process. This results in a wave-mixing induced transparency and a nonhyperbolic quasi-matter-wave soliton that opens new research opportunities in hydrodynamic fluid research of degenerate quantum gases, such as phonon scattering in a two-dimensional sonic black hole horizon.

Atomic quantum gases describe a class of atomic vapors at extremely low temperatures where microscopic quantum properties of the ensemble exhibit themselves on the macroscopic level [1]. Since their first demonstrations [2–4] over twenty years ago, quantum gases have been the most active subject of study in atomic physics. The main research objectives with quantum gases focus on collective effects and their direct correspondence with well known processes in condensed matter physics. While many seminal theoretical and experimental findings have been reported in this area, most do not contradict conventional knowledge in condensed matter physics [5]. Because of this, so far, atomic quantum gases have proven to be mostly a more accurate and robust platform for testing already known processes and effects in condensed matter physics.

The impact of quantum gases on nonlinear optics [6], however, is much more profound and fundamental. Recently, it has been shown that, not only do highly efficient multi-wave-mixing processes occur in directions not allowed in thermal gases [7–9], but the Bogoliubov spectra of spin-preserving optical processes exhibit highly nonlinear onsets and cutoffs in the phonon regime [10], a drastic departure from the well-known Feynman relation. These studies show that high-order optical processes can profoundly couple to the fundamental excitations, resulting in new effects that are strongly forbidden in thermal gases and nonquantum-degenerated solid-state materials. Indeed, nonlinear optics and condensed matter physics now become intimately coupled in the context of quantum-degenerated systems. In this work, we show an intriguing and unexpected nonlinear optical effect in quantum gases that does not have a correspondence in thermal gases. We

show that a nonhyperbolic matter solitonic wave arises from a novel optical wave mixing induced transparency.

Among the many exotic properties of quantum gases is the atomic center-of-mass (c.m.) motion which is completely negligible in thermal gases. Nonlinear optics of a quantum gas must be formulated using the Gross-Pitaevskii equation [1] for the collective response of the system in conjunction with Maxwell's equations describing the generation and propagation of light fields. Here, we consider a column of atomic quantum gas [Fig. 1(a)] that is under excitation by a pump field with wave vector k_L. For simplicity, we focus on the process in which three pump
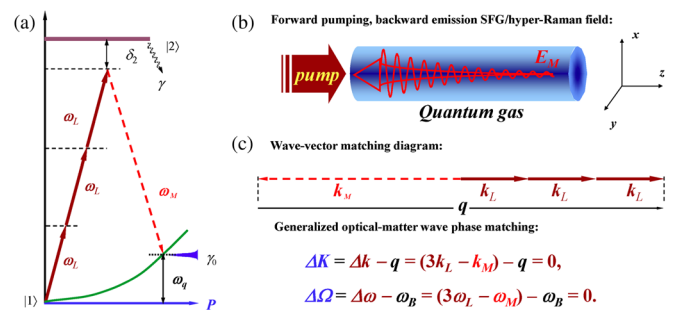

FIG. 1. Energy levels and matter-optical energy-momentum conservation. (a) Energy level diagram with laser coupling for three-photon hyper-Raman generation. (b) Colinear pumping geometry for the backward generation of hyper-Raman mixing wave. (c) Wave vector diagram showing combined matter-optical wave phase matching. Optical wave vector and energy mismatch are given by $\Delta \vec{k} = 3\vec{k}_L - \vec{k}_M$ and $\Delta \omega = 3\omega_L - \omega_M$. The atomic quasimomentum and total recoil energy are $\hbar \vec{q}$ and $\hbar \omega_R = (\hbar q)^2/(2M)$.

photons at frequency ω_L [11] propagating along the long axis of the quantum gas are simultaneously absorbed, and a photon of frequency ω_M is emitted in the direction opposite to the pump field [7–9]. As a result of this three-photon excitation process, a total of $\hbar q = 6\hbar k_L$ momentum is transferred to the atom, causing it to move with a center-of-mass velocity $\sim 6v_{\rm rec}$ [$v_{\rm rec}$ is the single photon recoil velocity, see Figs. 1(b) and 1(c) for phase matching conditions].

In the Maxwell-Bogoliubov formalism [8,12], the atomic mean-field wave function is given by [1,13,14],

$$\Psi(\mathbf{r}, t) = e^{i\mu t}[\Psi_0(\mathbf{r}) + ue^{i(\mathbf{q}\cdot\mathbf{r}-\omega_\mathbf{q}t)} + v^*e^{-i(\mathbf{q}\cdot\mathbf{r}-\omega_\mathbf{q}t)}]. \quad (1)$$

Here, $\Psi_0(\mathbf{r})$ is the ground state atomic mean-field wave function in the absence of external fields, and $\mu = g|\Psi|^2$ is the chemical potential with $g = 4\pi\hbar^2 a_S/M$, a_S and M are the s-wave scattering length and the atomic mass, respectively. In general, Eq. (1) obtained from a linearized fluctuation analysis should also include multiple momentum and corresponding Bogoliubov frequency modes. However, in the present case, the dominant scattering is a first-order momentum transfer process which already introduces a large c.m. velocity to collectively scattered atoms, resulting in a substantial Doppler frequency shift that significantly suppresses any higher-order scattering contributions. Correspondingly, effects due to the Bogoliubov phonon frequency distribution are negligible. It is, therefore, sufficient to focus only on this first-order hyper-Raman generation process.

Inserting Eq. (1) into the trap-free [15] Gross-Pitaevskii equation describing the evolution of the quantum gas under excitation, i.e.,

$$i\hbar\frac{\partial\Psi}{\partial t} = \left(-\frac{\hbar^2}{2M}\nabla^2 + g|\Psi|^2\right)\Psi$$
$$+ (\hbar\beta e^{-i\Delta\mathbf{k}\cdot\mathbf{r}+i\Delta\omega t} + {\rm H.c.})\Psi, \quad (2)$$

we obtain the following equations of motion characterizing quantum gas density fluctuations:

$$\frac{\partial}{\partial t}\begin{pmatrix} u \\ v \end{pmatrix} = \begin{pmatrix} \mathcal{A}_- & -iB \\ iB & \mathcal{A}_+ \end{pmatrix}\begin{pmatrix} u \\ v \end{pmatrix} + i\begin{pmatrix} -1 \\ 1 \end{pmatrix}\beta^*\Psi_0. \quad (3)$$

In deriving Eq. (3), we defined $\mathcal{A}_\pm = -\gamma_0 + i\omega_\mathbf{q} \pm iA$ and $A = \omega_\mathbf{q} + 2g|\Psi_0|^2/\hbar - \mu$, $B = g\Psi_0^2/\hbar$ with $\hbar\mathbf{q}$ and $\hbar\omega_\mathbf{q} = \hbar^2 q^2/2M$ being the quasimomentum and the corresponding atomic c.m. recoil energy induced by the light scattering process, respectively. In addition, the nonlinear coupling parameter is $\beta = \Omega_M\Omega_P^{(3)*}/\Delta_2$ [$\Delta_2 = \delta_2 + i\gamma_2$, see Fig. 4(a)]. $\Omega_M = d_{12}\cdot\mathbf{E}_M/\hbar$ is the Rabi frequency of the hyper-Raman field and $\Omega_P^{(3)}$ is the three-photon pumping Rabi frequency of the mixing-wave generating state. We note that β, being dependent on the generated field Ω_M, is nonlinear and dynamically changing as a function of the

propagation distance, and this introduces rich dynamics that cannot be produced by a simple two-photon Raman process. We also introduced a phenomenological momentum state resonance line width γ_0 which characterizes the damping of elementary excitations. This quantity, which plays a critical role in high-gain wave generation in quantum gases, has already been measured experimentally using a Bragg scattering technique [16].

The Maxwell-Bogoliubov equation of motion governing the quasi-one-dimensional coherent propagation growth of the hyper-Raman field is given by [7]

$$\frac{\partial\Omega_M}{\partial z} = \frac{i\kappa_{12}\Omega_M}{\Delta_2}\left[|\Psi_0|^2 + |u|^2 + |v|^2 + \frac{\Omega_P^{(3)}}{\Omega_M}(u^* + v^*)\Psi_0\right]. \quad (4)$$

The source term on the right side consists of three contributions. The $|\Psi_0|^2$ term is the usual linear absorption, as in a thermal gas. The additional nonlinear terms $|u|^2 + |v|^2$ arise from collective excitations of the quantum gas. The last term describes the multi-wave-mixing process arising from fundamental collective excitations [17]. In deriving Eqs. (3) and (4), we defined and enforced generalized phase-matching conditions that encompass both the matter and optical waves, i.e., $\Delta\mathbf{K} = \mathbf{q} - \Delta\mathbf{k} = 0$ and $\Delta\Omega = \Delta\omega - \omega_\mathbf{q} = 0$ [Figs. 1(b) and 1(c)]. Here, $\Delta\mathbf{k} = 3\mathbf{k}_L - \mathbf{k}_M$ and $\Delta\omega = 3\omega_L - \omega_M$ are the usual optical wave vector and energy mismatches between the pump and hyper-Raman fields.

For mathematical simplicity, and without the loss of generality, we consider the first-order solution of Eq. (3) by taking $\dot{u} = 0$, $\dot{v} = 0$. We obtain

$$\begin{pmatrix} u \\ v \end{pmatrix} = \frac{i}{D}\begin{pmatrix} \mathcal{A}_+ - iB \\ -\mathcal{A}_- - iB \end{pmatrix}\beta^*\Psi_0 e^{-i\xi}, \quad (5)$$

where $D = \mathcal{A}_+\mathcal{A}_- - B^2$. We emphasize, however, that we have solved Eqs. (3) and (4) numerically without any approximations and obtained the same results, thereby validating the approximations used in obtaining Eq. (5).

Substituting Eq. (5) into Eq. (4) yields

$$\frac{\partial\Omega_M}{\partial z} = i\tilde{\phi}\Omega_M + (G - \alpha)\Omega_M, \quad (6)$$

where the nonlinear hyper-Raman-like gain coefficient is $G = 4\kappa_{12}\mathcal{R}_S/(\gamma_0\gamma_2)$ and the three-photon excitation rate is $\mathcal{R}_S = |\Omega_P^{(3)}|^2\gamma_2/4|\Delta_2|^2$. The total propagation phase $\tilde{\phi}$ and attenuation coefficient α are defined as

$$\tilde{\phi} = \frac{\kappa_{12}\delta_2}{|\Delta_2|^2}\left(1 + \frac{4\mathcal{R}_S|\Omega_M|^2}{\gamma_2\gamma_0^2}\right) = (\phi_0 + \phi_1|\Omega_M|^2),$$

$$\alpha = \frac{\kappa_{12}\gamma_2}{|\Delta_2|^2}\left(1 + \frac{4\mathcal{R}_S|\Omega_M|^2}{\gamma_2\gamma_0^2}\right) = (\alpha_0 + \alpha_1|\Omega_M|^2).$$

Here, $\phi_0 = \kappa_{12}\delta_2/|\Delta_2|^2$ and $\alpha_0 = \kappa_{12}\gamma_2/|\Delta_2|^2$ are the linear propagation phase and absorption coefficient. ϕ_1 and α_1 are the dynamic nonlinear phase shift and absorption coefficient resulting from fundamental excitations which give rise to new nonlinear optical effects that do not exist in a thermal gas.

In a thermal gas, a hyper-Raman-like emission process requires that the gain must be larger than the overall static absorption to ensure coherent propagation growth of the hyper-Raman field. However, this is not sufficient in the case of a quantum gas. Equation (6) indicates that a dynamic absorption arising from the hyper-Raman-dependent fundamental excitation (α_1) can, under suitable excitation conditions, cancel the highly efficient hyper-Raman gain. As a result, a gain cancellation effect occurs, and growth of the backward hyper-Raman field becomes independent of both the density and the propagation distance of the quantum gas.

Defining $\mathcal{G} = G - \alpha_0 > 0$ and letting $\Omega_M = Re^{i\phi}$, where $R = |\Omega_M|$ and ϕ are real quantities, Eq. (6) becomes

$$\frac{\partial}{\partial z}\begin{pmatrix} R \\ \phi \end{pmatrix} = \begin{pmatrix} \mathcal{G}R - \alpha_1 R^3 \\ \phi_0 + \phi_1 R^2 \end{pmatrix}. \tag{7}$$

Neglecting the longitudinal density distribution, the first equation in Eq. (7) yields an analytical solution

$$R^2 = |\Omega_M|^2 = \frac{R_0^2 e^{2\mathcal{G}z}}{1 + QR_0^2(e^{2\mathcal{G}z} - 1)}, \tag{8}$$

where $Q = \alpha_1/\mathcal{G}$, and $R_0^2 = |\Omega_M^{(0)}|^2$ is proportional to the intensity of the initial seed photon of frequency ω_M propagating in the backward direction. For weak coherent propagation growth (such as in the initial growth, small propagation distances, low atomic density, or large pump detunings and weak excitation), Eq. (8) reduces to the well-known hyper-Raman intensity growth characteristics in a quantum gas $R^2 = R_0^2 e^{2\mathcal{G}z}$ [8].

Under high gain operations, however, there is a unique backward propagation regime that does not have any correspondence in a thermal gas. In this regime, $QR_0^2 e^{2\mathcal{G}z} \gg 1$ (typical experimental gain is $> 10\,e$ fold), and Eq. (8) reduces to $R^2 \to 1/Q = (\gamma_0/\gamma_2)|\delta_2|^2$. This relation contains two predictions. (1) When the gain cancellation effect occurs, the hyper-Raman field generation is independent of both density and propagation distance. (2) In this regime, the hyper-Raman photon production can be achieved by independently increasing the detuning from the resonance without changing the excitation rate $\mathcal{R}_S$. The first prediction is obvious since the gain, which depends on the product of the density and propagation distance, is fully canceled in this regime. If a light field of the same frequency ω_M as the hyper-Raman field were injected into a medium prepared in this manner, it would experience no change in intensity, just as if the medium were not present. This is a multiphoton wave

mixing induced transparency (WMIT). It is, however, important to note that, while the density and propagation-independent properties resulting from WMIT effects in a quantum gas are similar to those of electromagnetically induced transparency (EIT) [18] and well known multi-photon destructive interference effects [19–27] in a thermal gas, they are fundamentally different. The aforementioned effects are the result of interference between amplitudes of different excitation pathways and channels. Clearly, the hyper-Raman gain cancellation effect is not an interference effect.

The second prediction can be understood by examining the pump detuning dependency of the dynamic balance process. Notice that the scattering rate $\mathcal{R}_S$ and linear absorption α_0 both scale as $1/|\Delta_2|^2$. However, the dynamic absorption scales $1/|\Delta_2|^4$. Therefore, within a certain range of δ_2 (numerically, we found this range to be about 100 MHz [28]), under a constant scattering rate, the reduction of pump detuning actually results in a relative gain increase since α_1 decreases much faster.

As a numerical example, we consider a quantum gas with a uniform distribution and density $n = 10^{14}/\text{cm}^3$, with $\gamma_0/2\pi = 20$ kHz, $\kappa_{12} = 5 \times 10^{10}/(\text{cm}\cdot\text{s})$, $\gamma_2/2\pi = 10^7$ Hz, and $\delta_2/2\pi = 200$ MHz (so that $\gamma_2/\delta_2 < 0.05$). Assuming there is one initial photon traveling backward along the long axis with Rabi frequency $R_0 = 2\pi \times 3.14$ kHz (for a 100 μs pulse in a 20 μm gas column diameter), and letting $QR_0^2 e^{2\mathcal{G}z_c} \approx 10$ estimate the propagation length under a three-photon pump rate of $\mathcal{R}_S \simeq 35$ kHz so the gain cancellation effect becomes pronounced, we obtain an estimate of the propagation depth at which the cancellation effect dominates. Furthermore, by integrating the second half of Eq. (7), we obtain the phase of the hyper-Raman field in the gain cancellation regime

$$\phi(z) \approx \phi_0\left(1 + \frac{4\mathcal{R}_S}{\gamma_4\gamma_0^2 Q}\right)z + \text{const}, \tag{9}$$

where ϕ_0 is given after Eq. (6). This result indicates that the phase of the generated field initially increases linearly in z with a slope ϕ_0.
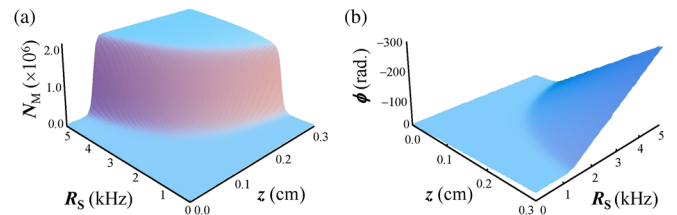

FIG. 2. WMIT in a bosonic quantum gas. (a) Photon numbers showing production saturation limited by the gain cancellation effect [see Eq. (8)]. (b) The gain cancellation effect develops from the center and grows radially outward. The linear growth of the phase of the wave-mixing field after the cancellation effect occurs [see Eq. (9)].
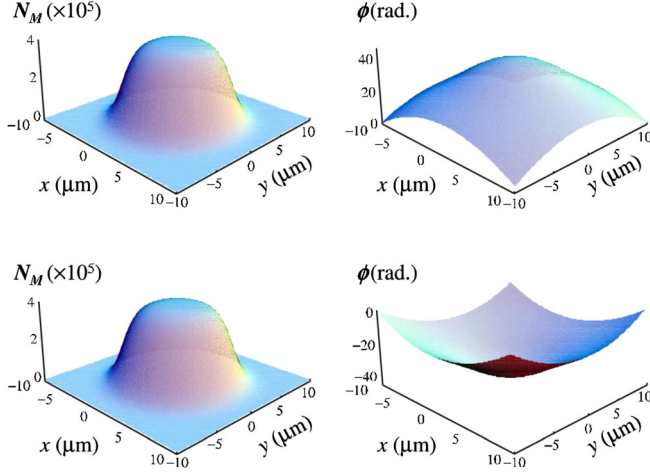
FIG. 3.   Propagation phase flip for different laser detunings in a bosonic quantum gas. Photon numbers showing production saturation limited by the gain cancellation effect and a positive phase with blue detuning (top) and a negative propagation phase shift from a red-detuned laser (bottom).

FIG. 4.   WMIT in a bosonic quantum gas without any propagation phase. (a) Energy level diagram: a doublet excited state and laser couplings ($\gamma_{41} = \gamma_{42} = \gamma$). (b) Top: Photon number distribution across the exit plane of an elongated Bose condensate. Bottom: The cancellation of the total propagation phase by a hyperfine doublet such as the D_1 transitions of rubidium atoms.

In Fig. 2, we plot the intensity [Fig. 2(a)] and propagation phase [Fig. 2(b)] of the backward-emitted hyper-Raman field as a function of the excitation rate $\mathcal{R}_S$ and propagation distance z. Here, the medium is assumed to be a bosonic quantum gas with a uniform density distribution. The photon production initially increases exponentially but later becomes propagation-distance and density independent.

When the Thomas-Fermi distribution of a trap-released bosonic quantum gas is included, the gain cancellation effect develops first in the center along the long axis [we take $n = n_0(1 - r^2/r_0^2)$, where n_0 and r_0 are the peak density and transverse Thomas-Fermi radius]. As the propagation distance increases, gain cancellation develops radially outward, and for a sufficient propagation distance, the intensity distribution of the generated light field across the quantum gas becomes flat, heralding the distance and density independent propagation of the hyper-Raman field. If a field of the same frequency ω_M is injected along the long axis, it will propagate unimpeded, as if the medium is not present, effectively experiencing a wave-mixing-induced transparency.

Equation (9) indicates that the optical field propagation phase depends linearly on the three-photon pump detuning in the gain cancellation regime. Thus, the sign change of the propagation phase can be achieved by changing the sign of the pump detuning (Fig. 3). This indicates that a WMIT scheme without a propagation phase can be achieved by carefully choosing two adjacent excited atomic states [Fig. 4(a)]. In this case, suitable van der Waals coefficient C_3 contributions from the two channels with opposite detunings leads to a complete cancellation of the total propagation phase [Fig. 4(b)]. We note that an interference-based induced transparency with zero-phase propagation can only be achieved with an EIT scheme that relies on
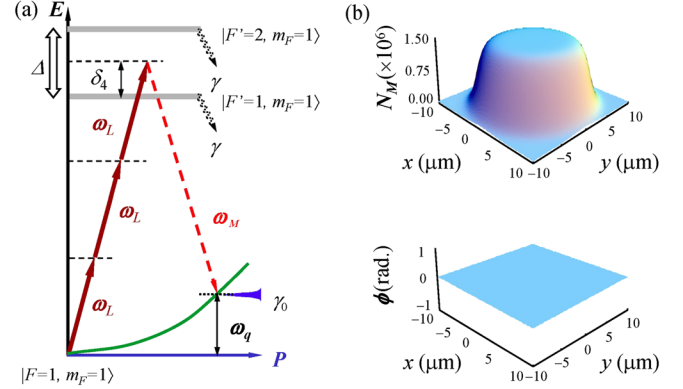
destructive interference between amplitudes of different excitation pathways. The WMIT with zero propagation phase shown here is based on very different physical principles. It is interesting to point out that, in this regime, the WMIT process results in a new type of matter-wave soliton [29,30] that cannot be produced with the usual matter-wave nonlinear Schrödinger equation.
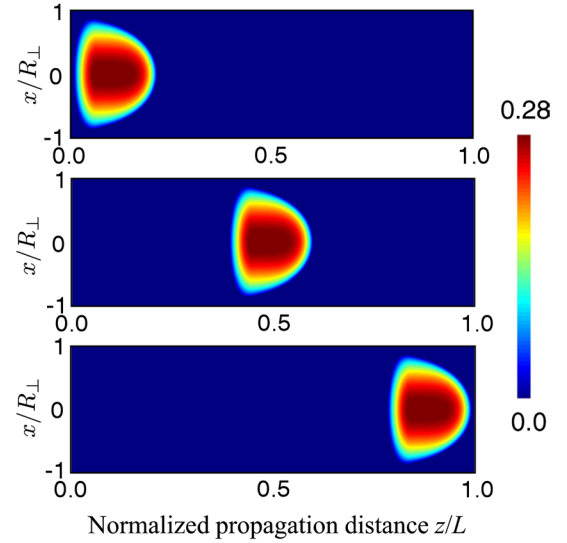

FIG. 5.   Propagation of a nonhyperbolic matter-wave quasisolitary wave created by WMIT of hyper-Raman light field generation. The color scale represents the moving matter wave density distribution normalized over the initial condensate peak density. Top: A flat-top matter-wave soliton is created at the end where the WMIT is effective and WM saturates. Middle: $t \simeq 6$ ms after the excitation. Bottom: $t \simeq 12$ ms after the excitation. The curved matter-wave front creates a moving superfluid that may have applications in analog hydrodynamics and astrophysics research.

Figure 5 shows a matter-wave soliton that was created when the WMIT is effective. The medium is an elongated condensate with a transverse distribution that has a Thomas-Fermi radius of $R_\perp$, and a constant longitudinal distribution that begins to drop quadratically near each end. Such a system can be readily created using an optical dipole trap supplemented with two blue-detuned laser caps at each end. When the hyper-Raman field saturates due to the presence of WMIT, the growth of the matter wave also saturates, giving rise to a nonhyperbolic matter-wave soliton that does not have diffraction-resulted ripples in its front edge [29]. Such a moving (∼12 mm/s for ^{87}Rb $5P$ state), two-dimensional matter solitonic wave with a uniform curved wave front may lead to intriguing hydrodynamic effects such as turbulence in superfluid and phonon scatterings near a two-dimensional curved sonic "black hole horizon" that does not appear in one-dimensional sonic fluids created mechanically.

The wave-mixing induced transparency described above should also occur in a degenerate fermion quantum gas but at higher pump rates and longer propagation distances. This is partially because the Fermi temperature of degenerate fermions is higher, resulting in a much broader momentum state resonance line width γ_0 and, therefore, much lower coherent propagation gain. It should be noted, however, that, while optical-matter wave mixing processes occur in both bosonic and fermionic quantum gases, an additional molecular process due to light-assisted ultracold collision can result in very different coherent propagation gain in these two types of quantum gases. The Pauli exclusion principle precludes the formation of a molecule from a single-component atomic fermion gas via photoassociation, whereas such a process occurs efficiently in a bosonic quantum gas. In addition, not all lower transitions accessible experimentally can lead to a high-gain wave-mixing process with bosonic quantum gases when the pump is blue-detuned with respect to the wave-mixing transition. It has been shown that the gradient of the van der Waals potential and the spontaneous emission time of the transition involved can critically impact a high-gain wave-mixing process [31–33]. This points to the interesting possibility of using nonlinear light-matter wave-mixing processes and the WMIT effect to probe molecular processes and potentials in quantum gases.

Atomic quantum gases present exciting new research opportunities in the field of nonlinear optics at weak light intensities. The light-matter wave interaction processes with atomic center-of-mass motion and coherent, collective matter-wave effects can lead to many new unexpected effects that might, otherwise, be strictly forbidden in nonlinear optics of thermal gases or solid-state materials. Quantum gas specific nonlinear optical effects such as the WMIT in the backward direction, the resulting matter solitonic waves, and the possible exotic matter-wave sonic horizon exemplify the novelty of this new research direction within the discipline of nonlinear optics.

[*] cjzhu@tongji.edu.cn
[†] lu.deng@nist.gov

[1] F. Dalfovo, S. Giorgini, L. P. Pitaevskii, and S. Stringari, Rev. Mod. Phys. **71**, 463 (1999).

[2] M. H. Anderson, J. R. Ensher, M. R. Matthews, C. E. Wieman, and E. A. Cornell, Science **269**, 198 (1995).

[3] K. B. Davis, M. O. Mewes, M. R. Andrews, N. J. van Druten, D. S. Durfee, D. M. Kurn, and W. Ketterle, Phys. Rev. Lett. **75**, 3969 (1995).

[4] C. C. Bradley, C. A. Sackett, and R. G. Hulet, Phys. Rev. Lett. **78**, 985 (1997).

[5] Quantum field theoretical treatment of an atomic-molecular condensate with fluctuations included has lead to predictions not previous realized. See, J. J. Hope and M. K. Olsen, Phys. Rev. Lett. **86**, 3220 (2001).

[6] Y. R. Shen, *The Principles of Nonlinear Optics* (John Wiley & Sons, Inc., New York, 1984).

[7] L. Deng, M. G. Payne, and W. R. Garrett, Phys. Rep. **429**, 123 (2006).

[8] L. Deng, C. J. Zhu, and E. W. Hagley, Phys. Rev. Lett. **110**, 210401 (2013).

[9] L. Deng, E. W. Hagley, R. Q. Wang, and C. W. Clark, Opt. Photonics News **24**, 44 (2013).

[10] Y. Li, C. J. Zhu, E. W. Hagley, and L. Deng, Sci. Rep. **6**, 25690 (2016).

[11] Experimentally, the $5S \rightarrow 5P_{3/2} \rightarrow 4D \rightarrow 5P_{1/2}$ pathway is readily accessible with diode lasers of moderate powers, resulting in very efficient three-photon excitation of the $5P_{1/2}$ state that has a strong one-photon coupling to the ground state.

[12] M. G. Moore and P. Meystre, Phys. Rev. Lett. **83**, 5202 (1999).

[13] F. Zambelli, L. P. Pitaevskii, D. M. Stamper-Kurn, and S. Stringari, Phys. Rev. A **61**, 063608 (2000).

[14] P. B. Blakie, R. J. Ballagh, and C. W. Gardiner, Phys. Rev. A **65**, 033602 (2002).

[15] In most light-quantum gas experiments the trapping potential is always turned off before the pump laser is switched on to avoid complications arising from the initial mean-field expansion.

[16] J. Stenger, S. Inouye, A. P. Chikkatur, D. M. Stamper-Kurn, D. E. Pritchard, and W. Ketterle, Phys. Rev. Lett. **82**, 4569 (1999).

[17] Electronic contributions to the hyper-Raman polarization have been neglected since they cannot be phase-matched in a single-species quantum gas.

[18] S. E. Harris, Phys. Today **50**, No. 7, 36 (1997).

[19] J. C. Miller, R. N. Compton, M. G. Payne, and W. R. Garrett, Phys. Rev. Lett. **45**, 114 (1980).

[20] M. G. Payne and W. R. Garrett, Phys. Rev. A **26**, 356 (1982).

[21] D. J. Jackson and J. J. Wynne, Phys. Rev. Lett. **49**, 543 (1982).

[22] C. Chen, Y. Y. Yin, and D. S. Elliott, Phys. Rev. Lett. **64**, 507 (1990).

[23] M. A. Moore, W. R. Garrett, and M. G. Payne, Phys. Rev. A **39**, 3692 (1989).

[24] Y. P. Malayakan, Opt. Commun. **69**, 315 (1989).

[25] R. K. Wunderlich, W. R. Garrett, R. C. Hart, M. A. Moore, and M. G. Payne, Phys. Rev. A **41**, 6345 (1990).

[26] W. R. Garrett, Phys. Rev. Lett. **70**, 4059 (1993).

[27] L. Deng, J. Y. Zhang, M. G. Payne, and W. R. Garrett, Phys. Rev. Lett. **73**, 2035 (1994).

[28] By adjusting laser parameters in a one- and two-photon resonantly enhanced excitation scheme ([11]), this region can be moved around, allowing the system to be tuned.

[29] J. Denschlag, J. E. Simsarian, D. L. Feder, W. C. Clark, L. A. Collins, J. Cubizolles, L. Deng, E. W. Hagley, K. Helmerson, W. P. Reinhardt, S. L. Rolston, B. I. Schneider, and W. D. Phillip, Science **287**, 97 (2000).

[30] L. Khaykovich, F. Schreck, G. Ferrari, T. Bourdel, J. Cubizolles, L. D. Carr, Y. Castin, and C. Salomon, Science **296**, 1290 (2002).

[31] L. Deng, E. W. Hagley, Q. Cao, X. R. Wang, X. Y. Luo, R. Q. Wang, M. G. Payne, F. Yang, X. J. Zhou, X. Z. Chen, and M. S. Zhan, Phys. Rev. Lett. **105**, 220404 (2010).

[32] X. Y. Luo, K. Y. Gao, L. Deng, E. W. Hagley, and R. Q. Wang, Phys. Rev. A **86**, 043603 (2012).

[33] N. S. Kampel, A. Griesmaier, M. P. Hornbak Steenstrup, F. Kaminski, E. S. Polzik, and J. H. Muller, Phys. Rev. Lett. **108**, 090401 (2012).